*Journal of Statistical Physics, Vol. 62, Nos. 5/6, 1991*

# Towards *ab Initio* Simulations of Concentrated Suspensions

**Sangtae Kim,[1] Yuris O. Fuentes,[1] and Seppo J. Karrila[2]**

*Received January 25, 1990; final July 9, 1990*

Determination of many-body interactions between particles of arbitrary shape in a viscous fluid is a key problem in the simulation of concentrated suspensions. Three-dimensional flows involving such complex fluid–solid boundaries are beyond the scope of spatial methods, even on supercomputers. Boundary integral methods convert the three-dimensional PDE to a two-dimensional integral equation. Unfortunately, conventional boundary methods yield Fredholm integral equations of the first kind, and dense linear systems which are too large for accurate solution. We have pursued a different boundary integral formulation, which yields Fredholm integral equations of the second kind; these are amenable to iterative solution. The velocity representation involves a compact operator, so a discrete spectrum results. Wielandt deflations give dramatic reductions in the spectral radius and accurate solutions are obtained after only a few iterations (typically less than 10). An analytic construction of the spectrum for sphere sphere interactions confirms these numerical results. The mathematics is similar to that encountered in the mixing of *d*-atomic orbitals to form bonding/antibonding molecular orbitals in transition metals. The memory-saving version of our code can be implemented directly on a dedicated MicroVAX to solve problems involving clusters of less than a dozen particles. For a fixed number of processors, the algorithm grows essentially as $N^2$, where $N$ is the system size, so computational times are readily estimated on more powerful super-minicomputers and supercomputers using standard "dot-product" benchmarks. The algorithm is especially ideal for gigaflop and teraflop parallel array processors under construction in a number of computer companies; an analysis of the spectrum reveals that asynchronous iterative methods will converge, leading the way to a rigorous formulation of screening concepts for suspended particles of arbitrary shape.

**KEY WORDS:** Suspensions; rheology; boundary integral method; parallel computing.

[1] Department of Chemical Engineering, University of Wisconsin, Madison, Wisconsin 53706.
[2] Paper Science Center, Finnish Pulp and Paper Research Institute, Espoo, Finland.



0022-4715/91/0300-1197$06.50/0 

## 1. INTRODUCTION

The interactions between submerged particles in a viscous problem are quite strong and long range in extent, decaying as $r^{-1}$ and $r^{-2}$, depending on whether the particles exert a net force on the fluid or not. A fast and accurate method for solving these $N$-body problems, for particles of arbitrary shape, in both bounded and unbounded flow domains clearly would be of great value in suspension simulation, either from the viewpoint of *ab initio* simulations, or for testing of popular approximations. Over the years, this lack of exact results has lead suspension theorists to develop a number of approximate approaches, the most important examples being cell models, periodic arrays, and self-consistent field theories. In addition, suspension simulations have simplified interactions using pairwise additivity and screening concepts. An overview of these approximations and the fair amount of success obtained in the modeling of suspensions of spheres is given in the review article by Brady and Bossis[1] and the book by Happel and Brenner.[2]

Over the past two years, our group at Wisconsin has developed a new approach to the problem of many-body interactions in a viscous fluid. The end results are numerical methods that can handle particles of arbitrary shape in both bounded and unbounded domains, and are based on fast iterative algorithms designed for conventional surpercomputers with vector operations, as well as parallel computers with multiple processors. An interesting aspect of this suspensions research is the central role played by a number of ideas from linear operator theory and numerical functional analysis. The fast iterative algorithms are intricately linked with these concepts and could not be devised otherwise. The velocity representations used in our work are not based on Green's identities, but instead stand on existence theorems of the Fredholm–Riesz–Schauder theory for integral equations with weakly singular kernels. Furthermore, the extraction of physical results such as the particle mobility, stresslet, and surface tractions is based on concepts from linear operator theory.

Two earlier articles (Karrila and Kim[3] and Karrila *et al.*[4]) derive most of the fundamental ideas used here. The first paper deals with the existence of the velocity representations, including numerical examples involving particles of extreme aspect ratios and sharp corners, while the second describes the development of iterative algorithms, especially those designed for parallel computers. The most complete (140 pages) exposition of this method may be found in Chapters 14–19 of *An Introduction to Microhydrodynamics* by Kim and Karrila.[5] In this article, we focus on those issues related to the application of the method to the solution of many-body mobility problems, to provide a permanent record of the presentation at this conference.

## 2. THE COMPLETED DOUBLE-LAYER BOUNDARY INTEGRAL EQUATION

Three-dimensional flow problems with complex moving boundaries, even if only for a small representative sample of concentrated suspension configurations, seem to be beyond the scope of spatial methods, such as finite elements and finite differences, in the foreseeable future (Fig. 1). Instead, we start with the governing Stokes equations for an incompressible Newtonian fluid of viscosity $\mu$,

$$-\nabla p + \mu \nabla^2 \mathbf{v} = 0, \qquad \nabla \cdot \mathbf{v} = 0 \tag{1}$$

and reformulate them as a two-dimensional (boundary) integral equation,

$$\mathbf{v}(\mathbf{x}) = -\frac{1}{8\pi\mu} \oint_S \mathbf{t}(\xi) \cdot \mathcal{G}(\mathbf{x} - \xi)\, dS(\xi) + \frac{1}{2} \oint_S \mathbf{K}(\mathbf{x} - \xi) \cdot \mathbf{v}_s(\xi)\, dS(\xi) \tag{2}$$

The unknowns correspond to the surface tractions $\mathbf{t} = \boldsymbol{\sigma} \cdot \mathbf{n}$ and surface velocities $\mathbf{v}_s$. Here, $\mathbf{n}$ is the surface normal pointing out of the particle and into the fluid. The symbol $\mathcal{G}$ denotes the Oseen tensor, the fundamental

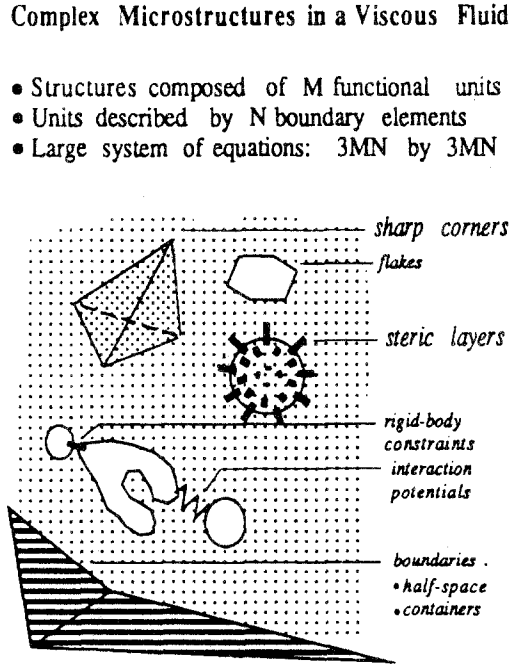


Fig. 1. Some difficult geometries encountered in suspension simulations.

solution or Green's function of the Stokes equations, which is given explicitly by

$$\mathscr{G}_{ij}(\mathbf{x}) = \frac{1}{|\mathbf{x}|}\delta_{ij} + \frac{1}{|\mathbf{x}|^3}x_i x_j \tag{3}$$

The integral representation given above has a long history dating back at least to Lorentz,[6] and numerical solution of the Stokes equations via discretization of this equation is also well known.[7] The two integral terms on the RHS of the integral representation are known as the single-layer and double layer potentials,[8] in analogy with the corresponding terminology in electrostatics. The kernel of the double-layer term is given by

$$\mathbf{K}(\mathbf{x}-\xi) = -2\mathbf{n}(\xi)\cdot\boldsymbol{\Sigma}(\mathbf{x}-\xi) \tag{4}$$

where $\boldsymbol{\Sigma}(\mathbf{x})$ is the stress field of $\mathscr{G}(\mathbf{x})/8\pi\mu$, or, more explicitly,

$$\boldsymbol{\Sigma}(\mathbf{x}) = -\frac{3}{4\pi}\frac{\mathbf{xxx}}{|\mathbf{x}|^5} \tag{5}$$

We define $\mathbf{K}$ with the factor of 2 so that its eigenvalues will be between $\pm 1$, as shown presently. When the boundary velocities are provided, the integral equation becomes a *Fredholm integral equation of the first kind* with the tractions as the unknown density.

The reduction in dimensionality represents a significant advantage in numerical solution of the Stokes equation. However, a direct application of this boundary integral formulation is not feasible for two important classes of hydrodynamic problems: geometries with sharp surface curvatures[9] and many-body problems. Indeed, this observation is a well-known result from the theory of linear operators and integral equations. The single-layer integral operator is *compact*, and in infinite-dimensional Hilbert spaces, the inverse of a compact operator is unbounded. Thus, in the sense of Hadamard, Fredholm equations of the first kind are *ill-posed*, since very different inputs are mapped by the compact operator to very similar outputs. This ill-posedness is not apparent in problems where coarse meshes yield acceptable results, such as flow past a single sphere.[7]

Now first consider a boundary geometry possessing sharp curvatures, either in the form of grooves and protrusions on a single particle surface, or in the form of narrow necks of interstitial regions formed by particles near contact. Then the ill-posedness of the Fredholm integral equation of the first kind cannot be avoided. The ratio of the largest (normwise) to smallest eigenvalue becomes increasingly large with increasing surface curvature and narrowing neck thickness. For example, for two spheres near

contact, this ratio scales as $O(n)$, where $n$ is the number of terms retained in the twin-multipole expansion representation of the two-sphere velocity field.[5] Naturally, discretization of an ill-posed problem encounters the associated problem of ill-conditioning, and since the solutions of interest for two almost-touching particles contain highly oscillatory components, regularization procedures are not easily implemented.

Second, consider many-body problems or any other situation where a large number of boundary elements is required to resolve the surface shape in a faithful manner. The solution of dense systems of the kind obtained above is an expensive proposition. On the other hand, our formulation of the boundary integral equation is amenable to fast iterative solutions. Indeed, large systems on the order of 10,000 by 10,000 have been solved without difficulty on minicomputers, and larger systems on the order of 1,000,000 by 1,000,000 are easily solved on conventional supercomputers. Since the method allows tradeoffs between processor workloads and memory usage, the future potential of this method is limited only by economic constraints on the design of new advanced computer architectures.

What follows is a summary of the development of our alternate integral representation for flow past a single particle, which leads to a *Fredholm equation of the second kind*, an idea first espoused by Power and Miranda.[10] We then discuss how this idea can be extended to multiparticle settings in both bounded and unbounded flows. We then present a summary of an iterative method for solving the resulting second-kind equations, with more details given in a subsequent section.

From Odqvist's work[8] we know that the double-layer potential is discontinuous at the surface. Specifically, the jump is exactly twice the local value of the the double-layer density, so that at the point $\mathbf{x}$ on the surface,

$$\lim_{\varepsilon \to 0} \left\{ \oint_S \mathbf{K}(\mathbf{x} + \varepsilon \mathbf{n} - \xi) \cdot \boldsymbol{\varphi}(\xi)\, dS(\xi) \right\} = \boldsymbol{\varphi}(\mathbf{x}) + \oint_S \mathbf{K}(\mathbf{x} - \xi) \cdot \boldsymbol{\varphi}(\xi)\, dS(\xi) \tag{6}$$

$$\lim_{\varepsilon \to 0} \left\{ \oint_S \mathbf{K}(\mathbf{x} - \varepsilon \mathbf{n} - \xi) \cdot \boldsymbol{\varphi}(\xi)\, dS(\xi) \right\} = -\boldsymbol{\varphi}(\mathbf{x}) + \oint_S \mathbf{K}(\mathbf{x} - \xi) \cdot \boldsymbol{\varphi}(\xi)\, dS(\xi) \tag{7}$$

Clearly, an integral representation based on just the double-layer potential alone,

$$\mathbf{v}(\mathbf{x}) = \oint_S \mathbf{K}(\mathbf{x} - \xi) \cdot \boldsymbol{\varphi}(\xi)\, dS(\xi), \qquad \mathbf{x} \in V_f \tag{8}$$

after imposition of the no-slip boundary condition, $\mathbf{v}(\mathbf{x}) = \mathbf{v}_s(\mathbf{x})$, $\mathbf{x} \in S$, yields the boundary integral equation,

$$\mathbf{v}_s(\mathbf{x}) = \boldsymbol{\varphi}(\mathbf{x}) + \oint_S \mathbf{K}(\mathbf{x} - \xi) \cdot \boldsymbol{\varphi}(\xi)\, dS(\xi), \qquad \mathbf{x} \in S \tag{9}$$

This is a Fredholm integral equation of the second kind. Unfortunately, most flows of interest do not fall into this category, because the double-layer potential alone cannot represent flows that exert a net hydrodynamic force or torque on the submerged body. This is precisely why the single-layer potential is needed in Lorentz's representation. The key idea in the work of Power and Miranda is that the single-layer potential may be replaced with the velocity fields of a point force and point torque, leading to an integral representation of the form

$$\mathbf{v}(\mathbf{x}) = -\mathbf{F}^{\mathrm{Hyd}} \cdot \frac{\mathscr{G}(\mathbf{x})}{8\pi\mu} - \mathbf{T}^{\mathrm{Hyd}} \times \frac{\mathscr{H}(\mathbf{x})}{8\pi\mu} + \oint_S \mathbf{K}(\mathbf{x}-\xi) \cdot \boldsymbol{\varphi}(\xi)\, dS(\xi) \tag{10}$$

Here, $\mathbf{F}^{\mathrm{Hyd}}$ and $\mathbf{T}^{\mathrm{Hyd}}$ are the hydrodynamic force and torque on the particle,

$$\mathbf{T}^{\mathrm{Hyd}} \times \mathscr{H}(\mathbf{x}) = \mathbf{T}^{\mathrm{Hyd}} \times \frac{\mathbf{x}}{|\mathbf{x}|^3} \tag{11}$$

is the field of a rotlet or point torque, and $\boldsymbol{\varphi}(\xi)$ represents the unknown double-layer density which is to be found. The operator notation,

$$\mathscr{K}(\boldsymbol{\varphi}) = \oint_S \mathbf{K}(\mathbf{x}-\xi) \cdot \boldsymbol{\varphi}(\xi)\, dS(\xi)$$

will be used for the last term in the boundary integral equation.

Note that this introduces six new unknowns (the three components of the force and torque). However, as we would expect from the *Fredholm alternative*, the null space of $1+\mathscr{K}$ is nontrivial; in fact, $N(1+\mathscr{K}) = R(1+\mathscr{K}^*)^{\perp}$ and since there are six "independent things" missing from the range $[\dim R(1+\mathscr{K}^*)^{\perp} = \dim R(1+\mathscr{K})^{\perp} = 6]$ there should be six linearly independent nontrivial null solutions of the equation $\boldsymbol{\varphi} + \mathscr{K}(\boldsymbol{\varphi}) = 0$. These are in fact the six independent rigid-body motions of the particle surface. The removal of this degeneracy provides exactly the right number of new equations, thus providing a unique solution. Instead of this interpretation, Power and Miranda chose to associate

$$F_i^{\mathrm{Hyd}} = -\oint \mathbf{e}_i \cdot \boldsymbol{\varphi}(\xi)\, dS(\xi) = -\langle \mathbf{e}_i, \boldsymbol{\varphi}(\xi) \rangle \tag{12}$$

$$T_i^{\mathrm{Hyd}} = -\oint (\mathbf{e}_i \times \xi) \cdot \boldsymbol{\varphi}(\xi)\, dS(\xi) = -\langle \mathbf{e}_i \times \xi, \boldsymbol{\varphi}(\xi) \rangle \tag{13}$$

and the bulk of the original article deals with the proof that the linear operator

$$\sum_{j=1}^{3}\left(\mathbf{e}_j\langle\mathbf{e}_j,\bullet\rangle\cdot\frac{\mathscr{G}(\mathbf{x})}{8\pi\mu}+\mathbf{e}_j\langle\mathbf{e}_j\times\xi,\bullet\rangle\times\frac{\mathscr{R}(\mathbf{x})}{8\pi\mu}\right)+\mathscr{K}$$

possesses a unique inverse.

The broader former interpretation, using the dimensions of the various subspaces associated with $1+\mathscr{K}$, was first given by Karrila and Kim,[3] along with a number of different completion schemes for multiparticle problems in unbounded and bounded flows. The entire class of boundary integral equation methods based on the idea of completion of the double-layer operator, naturally, are called *completed double-layer boundary integral equation methods.*

The most interesting completion scheme occurs for *mobility problems* where the force and torque on each particle are specified, and the unknown particle motions are to be determined (this category of problems includes two important problems in suspension theory: determination of the tracer diffusion coefficient and determination of sedimentation velocity). For mobility problems, we write the boundary integral equation as

$$\mathbf{U}+\boldsymbol{\omega}\times\mathbf{x}=-\mathbf{F}^{\mathrm{Hyd}}\cdot\frac{\mathscr{G}(\mathbf{x})}{8\pi\mu}-\mathbf{T}^{\mathrm{Hyd}}\times\frac{\mathscr{R}(\mathbf{x})}{8\pi\mu}+\boldsymbol{\varphi}(\mathbf{x})+\mathscr{K}(\boldsymbol{\varphi}),\qquad \mathbf{x}\in S \tag{14}$$

where $\mathbf{U}+\boldsymbol{\omega}\times\mathbf{x}$ is the rigid-body motion to be determined. (For the sake of clarity, we have written the equation for just the single-particle problem.)

The system of equations is completed by adding the six extra conditions of the form

$$U_j=-\frac{\oint\mathbf{e}_j\cdot\boldsymbol{\varphi}(\xi)\,dS(\xi)}{\oint dS(\xi)} \tag{15}$$

$$(\boldsymbol{\omega}\times\mathbf{x})=-\sum_{j=1}^{3}(\mathbf{e}_j\times\mathbf{x})\frac{\oint(\mathbf{e}_j\times\xi)\cdot\boldsymbol{\varphi}(\xi)\,dS(\xi)}{\oint(\mathbf{e}_j\times\xi)\cdot(\mathbf{e}_j\times\xi)\,dS(\xi)} \tag{16}$$

The expressions appearing in the denominators have been introduced for normalization purposes. Insertion of these six equations into the boundary integral equation yields

$$\sum_{j=1}^{6}\boldsymbol{\varphi}^{(j)}\langle\boldsymbol{\varphi},\boldsymbol{\varphi}^{(j)}\rangle+\boldsymbol{\varphi}(\mathbf{x})+\mathscr{K}(\boldsymbol{\varphi})=\mathbf{F}^{\mathrm{Hyd}}\cdot\frac{\mathscr{G}(\mathbf{x})}{8\pi\mu}+\mathbf{T}^{\mathrm{Hyd}}\times\frac{\mathscr{R}(\mathbf{x})}{8\pi\mu} \tag{17}$$

or

$$\varphi(\mathbf{x}) + \mathscr{H}(\varphi) = \mathbf{F}^{\mathrm{Hyd}} \cdot \frac{\mathscr{G}(\mathbf{x})}{8\pi\mu} + \mathbf{T}^{\mathrm{Hyd}} \times \frac{\mathscr{R}(\mathbf{x})}{8\pi\mu} \tag{18}$$

The operator $\mathscr{H}$ defined above is obtained from *Wielandt deflations* of the double operator $\mathscr{K}$, since $\mathbf{e}_j$ and $\mathbf{e}_j \times \mathbf{x}$, $j = 1, 2, 3$, are the six null eigenfunctions of the operator $1 + \mathscr{K}$. We reserve the notation $\varphi^{(j)}$, $j = 1, \ldots, 6$, for the orthonormalized null eigenfunctions, i.e., $\langle \varphi^{(j)}, \varphi^{(k)} \rangle = \delta_{jk}$.

This system of equations now has a unique solution. Further details of this version of CDL-BIEM, and the subtle details associated with the multiplicity of the eigenvalues and the necessary multiple Wielandt deflations, is presented in a later section, since it requires a detailed understanding of the spectrum of the double-layer operator in the more general many-body setting.

We conclude here by noting the advantages of the second-kind formulations over those based on the first kind. Upon discretization, the linear system from second-kind methods are well-conditioned, with very large elements on the diagonal—indeed, the ratio of off-diagonal to diagonal elements scales with the mesh size of the boundary integral method. Thus, while very fine scale discretizations inevitably lead to increased computational costs, this loss is partially offset by the increasing disparity between the diagonal and off-diagonal elements. Furthermore, the form of the second-kind equation usually leads to an iterative solution and these in turn are readily implemented on a wide range of computer architectures, including those from the rapidly developing field of parallel computers.

## 3. EXTRACTION OF PHYSICAL QUANTITIES

If we accept the premise that the most important objectives of the numerical calculations are the resistance/mobility relations, the surface tractions, and, in the case of bulk stress calculations, the stresslet on the particle, then postprocessing is clearly necessary with CDL-BIEM, for the double-layer density $\varphi$ obtained as the solution is not one of the primary physical quantities of interest. Fortunately, the completion procedure furnishes directly the resistance or mobility relations, as we have seen above. In fact, by picking as unknowns an appropriate pair from the set $(\mathbf{F}^{\mathrm{Hyd}}, \mathbf{T}^{\mathrm{Hyd}}, \mathbf{U}, \boldsymbol{\omega})$, we have the capability of solving any combination of resistance and mobility problems directly. This is important for suspension simulation work because the principle of first solving a canonical set of

resistance problems and then combining linearly to obtain the desired mobility or mixed problem becomes impractical in many-body systems.

In the following discussion, we show how the rest of the primary physical quantities of interest, surface tractions and stresslet, may be extracted from the CDL-BIEM solution.

### 3.1. Surface Tractions in Resistance Problems

For the special case of known rigid-body motion in the linear ambient field $\mathbf{v}^\infty = \mathbf{U}^\infty + \boldsymbol{\Omega}^\infty \times \mathbf{x} + \mathbf{E}^\infty \cdot \mathbf{x}$, Karrila and Kim[3,5] have shown that tractions can be obtained directly from the double-layer density, without resorting to the Newtonian constitutive equation for the stress (which requires differentiation of the velocity field). We show here how the tractions for a particle in steady translation are obtained. All others tractions in resistance problems are obtained in an analogous fashion.[5]

Using the Lorentz reciprocal theorem,[11] the drag on a particle in arbitrary ambient Stokes flow $\mathbf{v}^\infty$ may be expressed as

$$\mathbf{e}_i \cdot \mathbf{F}^{\mathrm{Hyd}} = \langle (\boldsymbol{\sigma}^{\mathrm{RBM}} \cdot \mathbf{n})^{(i)}, \mathbf{v}^\infty \rangle \tag{19}$$

where $(\boldsymbol{\sigma}^{\mathrm{RBM}} \cdot \mathbf{n})^{(i)}$ is the traction produced when the particle is in rigid-body translation in the $i$th coordinate direction.

If we interpret the preceding inner product as a linear functional mapping $\mathbf{v}^\infty$ to $\mathbf{F}^{\mathrm{Hyd}}$, then $(\boldsymbol{\sigma}^{\mathrm{RBM}} \cdot \mathbf{n})^{(i)}$ is the unique "vector" that performs this role (Riesz representation theorem of linear operator theory). However, the hydrodynamic force calculations in CDL-BIEM are always of the form

$$\mathbf{e}_i \cdot \mathbf{F}^{\mathrm{Hyd}} = \langle \mathbf{C}, \boldsymbol{\varphi} \rangle \tag{20}$$

with $\boldsymbol{\varphi} = \mathbf{A}^{-1}(\mathbf{v}^\infty)$, so that

$$\mathbf{e}_i \cdot \mathbf{F}^{\mathrm{Hyd}} = \langle \mathbf{C}, \mathbf{A}^{-1}(\mathbf{v}^\infty) \rangle = \langle (\mathbf{A}^{-1})^*(\mathbf{C}), \mathbf{v}^\infty \rangle \tag{21}$$

from which it follows that

$$(\boldsymbol{\sigma}^{\mathrm{RBM}} \cdot \mathbf{n})^{(i)} = (\mathbf{A}^{-1})^*(\mathbf{C}) \tag{22}$$

In Fig. 2, we show the agreement between the numerical implementation of this procedure and the analytical result (solid line) for the traction on a prolate spheroid. The two discrete curves indicate slightly different discretizations.

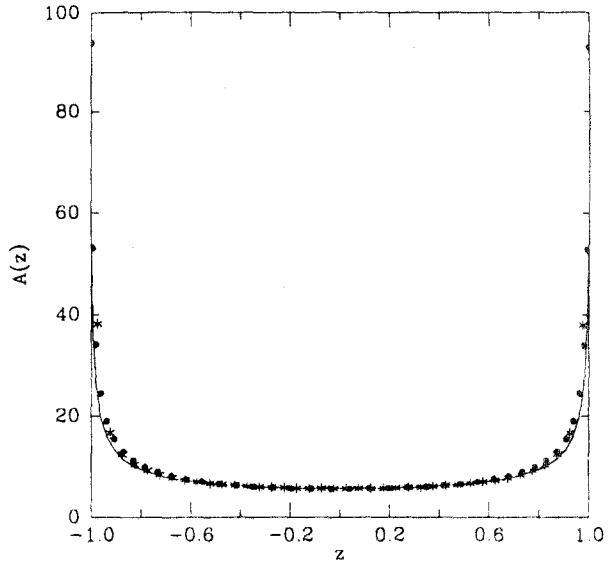


Fig. 2. The $x$ component of the traction, $\boldsymbol{\sigma}\cdot\mathbf{n} = A(z)\cos\phi$, on a prolate spheroid of aspect ratio 10 in transverse ($x$ direction) translation. The solid line is the analytical result.

## 3.2. Surface Tractions in Mobility Problems

Again, consider mobility problems where the force and torque on each particle are given, but the particle rigid-body motions relative to the linear ambient field $\mathbf{v}^{\infty} = \mathbf{U}^{\infty} + \boldsymbol{\Omega}^{\infty}\times\mathbf{x} + \mathbf{E}^{\infty}\cdot\mathbf{x}$ are to be determined. In such problems as well, the surface tractions can be obtained without differentiation of the numerical solution by use of the Riesz representation theorem.

Let $\mathbf{v}_s$ $(=-\mathbf{v}^{\infty})$ be a given velocity field on the particle surface, $\mathbf{v}^{\mathrm{RBM}}$ the velocity field corresponding to total force $\mathbf{F}^{\mathrm{Hyd}}$ and torque $\mathbf{T}^{\mathrm{Hyd}}$ (mobility solution), and $\mathbf{u}^{\mathrm{RBM}} = \mathbf{U} + \boldsymbol{\omega}\times\mathbf{x}$ be the RBM velocity such that the flow corresponding to the boundary condition $\mathbf{v}_s - \mathbf{u}^{\mathrm{RBM}}$ exerts no net force or torque on the particle.

The key step is an identity obtained from the Lorentz reciprocal theorem,

$$\langle \mathbf{u}, \mathbf{n}\cdot\boldsymbol{\sigma}(\mathbf{v}^{\mathrm{RBM}})\rangle = \mathbf{U}\cdot\mathbf{F}^{\mathrm{Hyd}} + \boldsymbol{\omega}\cdot\mathbf{T}^{\mathrm{Hyd}} \tag{23}$$

This shows the physical significance of mobility-based tractions—they map a given velocity field $\mathbf{v}_s$ to (components of) such an RBM which absorbs

the total force and torque, as claimed above. To derive this, we reason as follows:

$$\begin{aligned} 0 &= \langle \mathbf{n} \cdot \boldsymbol{\sigma}(\mathbf{v}_s - \mathbf{u}^{\mathrm{RBM}}), \mathbf{v}^{\mathrm{RBM}} \rangle \\ &= -\langle \mathbf{u}^{\mathrm{RBM}}, \mathbf{n} \cdot \boldsymbol{\sigma}(\mathbf{v}^{\mathrm{RBM}}) \rangle + \langle \mathbf{v}_s, \mathbf{n} \cdot \boldsymbol{\sigma}(\mathbf{v}^{\mathrm{RBM}}) \rangle \\ &= -(\mathbf{U} \cdot \mathbf{F}^{\mathrm{Hyd}} + \boldsymbol{\omega} \cdot \mathbf{T}^{\mathrm{Hyd}}) + \langle \mathbf{v}_s, \mathbf{n} \cdot \boldsymbol{\sigma}(\mathbf{v}^{\mathrm{RBM}}) \rangle \end{aligned}$$

It may be helpful to see how this works out for a single sphere. According to the Faxén law,[2] a force-free sphere or radius $a$, subject to the boundary condition $\mathbf{v}_s$, must translate as

$$\mathbf{U} = \left( \mathbf{v}_s + \frac{a^2}{6} \nabla^2 \mathbf{v}_s \right) \Big|_{x=0} = \frac{1}{4\pi a^2} \oint_{S_p} \mathbf{v}_s \, dS \tag{24}$$

so that

$$\mathbf{U} \cdot \mathbf{F}^{\mathrm{Hyd}} = \frac{1}{4\pi a^2} \oint_{S_p} \mathbf{u} \cdot \mathbf{F}^{\mathrm{Hyd}} \, dS = \frac{1}{4\pi a^2} \langle \mathbf{u}, \mathbf{F}^{\mathrm{Hyd}} \rangle \tag{25}$$

which correctly identifies

$$\boldsymbol{\sigma} \cdot \mathbf{n} = \frac{\mathbf{F}^{\mathrm{Hyd}}}{4\pi a^2}$$

as the surface tractions on a translating sphere on which a force $\mathbf{F}^{\mathrm{Hyd}}$ is exerted by the fluid. Again, to repeat the main theme: the Riesz theorem guarantees both the existence and uniqueness of these mobility-based RBM surface tractions in this role.

We now consider the link between this result and the boundary integral equation. Given a surface velocity field $\mathbf{v}_s$ that originated from a Stokes ambient field, we construct the mobility problem of a force-free and torque-free particle. The relevant boundary integral equation is

$$\sum_{j=1}^{6} \boldsymbol{\varphi}^{(j)} \langle \boldsymbol{\varphi}, \boldsymbol{\varphi}^{(j)} \rangle = -(1 + \mathscr{K}) \boldsymbol{\varphi} + \mathbf{v}_s \tag{26}$$

The Stokeslet and rotlet fields are absent from the boundary integral equation since the particle is force- and torque-free. The rigid-body motion (as yet unknown) has been replaced by the deflation terms, here represented in a condensed inner product notation in terms of the six null solutions, $\boldsymbol{\varphi}^{(j)}$.

The rigid-body motion is completely determined by the inner products on the LHS of the previous equation. Consider one such inner product. The mapping $\mathbf{v}_s \to \langle \boldsymbol{\varphi}, \boldsymbol{\varphi}^{(j)} \rangle$ is a linear functional, and thus by the Riesz

representation theorem, this image is of the form $\langle \mathbf{v}_s, \mathbf{t} \rangle$ for some fixed vector $\mathbf{t}$. We will see below that this is a traction for some rigid-body motion, $\mathbf{t} = \boldsymbol{\sigma}(\mathbf{V}^{\mathrm{RBM}})$, and then the only question that remains will be the identity of $\mathbf{V}^{\mathrm{RBM}}$. We fix $\mathbf{t}$ and insert arbitrary surface fields $\mathbf{u}$ in Eq. (26). If $\mathbf{u} \in R(1 + \mathscr{K})$, the RHS of Eq. (26) vanishes; therefore, so must the inner product on the LHS. Since this inner product also equals $\langle \mathbf{v}_s, \mathbf{t} \rangle$ by the definition of $\mathbf{t}$, we have the result $\mathbf{t} \perp R(1 + \mathscr{K})$, and therefore, from the *Fredholm alternative*, $\mathbf{t} \perp N(1 + \mathscr{K}^*)$. This identifies $\mathbf{t}$ as a traction from some rigid-body motion $\mathbf{V}^{\mathrm{RBM}}$, because Odqvist[8] has shown those are the only nontrivial null solutions of the adjoint operator. Now we identify $\mathbf{V}^{\mathrm{RBM}}$.

We take the inner product of $\mathbf{t}$ and both sides of Eq. (26) to obtain

$$\begin{aligned}\langle \mathbf{v}_s, \mathbf{t} \rangle &= \langle \boldsymbol{\varphi}^{(j)}, \mathbf{t}(\mathbf{V}^{\mathrm{RBM}}) \rangle \langle \boldsymbol{\varphi}, \boldsymbol{\varphi}^{(j)} \rangle \\ &= \sum_{j=1}^{3} (\mathbf{F}^{\mathrm{Hyd}} \cdot \boldsymbol{\varphi}^{(j)}) \langle \boldsymbol{\varphi}, \boldsymbol{\varphi}^{(j)} \rangle + \sum_{j=4}^{6} (\mathbf{T}^{\mathrm{Hyd}} \cdot \boldsymbol{\varphi}^{(j)}) \langle \boldsymbol{\varphi}, \boldsymbol{\varphi}^{(j)} \rangle\end{aligned}$$

where $\mathbf{F}^{\mathrm{Hyd}}$ and $\mathbf{T}^{\mathrm{Hyd}}$ are the force and torque (relative to the center of mass of the particle surface[5]) exerted by the fluid on the particle in rigid-body motion $\mathbf{V}^{\mathrm{RBM}}$.

We are now ready to extract tractions from mobility problems, using the previous result in the reverse way. For mobility problem with $\mathbf{F}^{\mathrm{Hyd}}$ and $\mathbf{T}^{\mathrm{Hyd}}$ given, we define

$$\boldsymbol{\varphi}_g = \sum_{j=1}^{3} \boldsymbol{\varphi}^{(j)} (\mathbf{F}^{\mathrm{Hyd}} \cdot \boldsymbol{\varphi}^{(j)}) + \sum_{j=4}^{6} \boldsymbol{\varphi}^{(j)} (\mathbf{T}^{\mathrm{Hyd}} \cdot \boldsymbol{\varphi}^{(j)}) \tag{27}$$

Then for *any* $\boldsymbol{\varphi}$, we have

$$\langle \boldsymbol{\varphi}, (1 + \mathscr{K}^*)\mathbf{t} \rangle = \langle (1 + \mathscr{K})\boldsymbol{\varphi}, \mathbf{t} \rangle = \langle \mathbf{v}_s, \mathbf{t} \rangle = \langle \boldsymbol{\varphi}, \boldsymbol{\varphi}_g \rangle \tag{28}$$

so that $\mathbf{t} = \mathbf{n} \cdot \boldsymbol{\sigma}(\mathbf{V}^{\mathrm{RBM}})$ can be solved from

$$(1 + \mathscr{K}^*)\mathbf{t} = \boldsymbol{\varphi}_g \tag{29}$$

As far as the discretized equations are concerned, this is just a simple matter of solving a second system of equations using the transpose of the system matrix from the original problem (mobility relation calculation). These ideas are readily extended to multiparticle problems.[5]

### 3.3. Stresslet for Bulk Stress Calculations

The traction calculations of the preceding sections apply only to rigid-body motions in a linear field. For tractions in *arbitrary* ambient Stokes

flow, there are no direct methods for the tractions using a second-kind formulation. This is readily established from the fact that second-kind equations involve operators that are compact perturbations of the identity, while the mapping from surface velocities to surface tractions involves an unbounded operator. Fortunately, the one moment of the surface traction which, together with the force and torque, is of great physical significance —the stresslet (or symmetric force dipole)—can also be obtained from the CDL-BIEM formulation.

The bulk stress ($\boldsymbol{\sigma}^{\text{eff}}$) in a suspension may be expressed as a sum of solvent ($\boldsymbol{\sigma}^{s}$) and particle contributions,[12]

$$\boldsymbol{\sigma}^{\text{eff}} = \boldsymbol{\sigma}^{s} + \langle n\mathbf{S} \rangle \tag{30}$$

where the stresslet $\mathbf{S}$ on each particle is defined by

$$\mathbf{S} = \frac{1}{2}\int_{S_p} [(\boldsymbol{\sigma}\cdot\mathbf{n})\boldsymbol{\xi} + \boldsymbol{\xi}(\boldsymbol{\sigma}\cdot\mathbf{n})]\, dS - \frac{\delta}{3}\int_{S_p} (\boldsymbol{\sigma}\cdot\mathbf{n})\cdot\boldsymbol{\xi}\, dS \tag{31}$$

The stresslet on any particle in the suspension can be obtained exactly from the double-layer density by the relation

$$\mathbf{S} = -2\mu \oint_{S} (\mathbf{n}\boldsymbol{\varphi} + \boldsymbol{\varphi}\mathbf{n})\, dS(\boldsymbol{\xi}) \tag{32}$$

where the surface integration is only over the particle of interest. The implementation of this work to suspension rheology is thus feasible. The derivation of the preceding result follows from an expansion of the double-layer potential in terms of the multiple series. The stresslet is simply the coefficient in the term that decays at $r^{-2}$.

## 4. ITERATIVE SOLUTIONS

It has been noted earlier that boundary integral equations lead to dense linear systems upon discretization. In contrast to spatial methods, where equations link only nearby neighboring nodes or elements and thus lead to sparse systems, the discrete equations in the boundary integral method link all elements, for the kernel in the integral equation is the Green's function (or its derivatives), and can propagate long distances through the fluid. Thus, when dealing with many-body problems, we face the prospect of solving very large, dense systems. For the sake of argument, consider a cluster of $N$ identical particles in an unbounded domain. If each particle is resolved by $M$ boundary elements, the system size is $3MN$ by $3MN$, and for $M = N = 100$, we already reach a size of 100,000 by 100,000—

and this is for just one configuration or time step. Iterative methods are the only realistic approach for the problem at hand.

Integral equations of the second kind lead to discretized systems of the form $x = Mx + b$, suggesting an obvious iterative algorithm. The convergence of iterative methods of the form

$$x_{n+1} = Mx_n + b \tag{33}$$

depends on the eigenvalues of $M$. The precise statement is that the iterations converge to the solution if and only if all eigenvalues of $M$ have norm less than one. If this condition is met, the rate of convergence is ultimately dictated by the largest eigenvalue. With each successive iteration, the "distance" of approximate solution $x_n$ from the actual solution will diminish by at least a factor equal to the norm of this dominant eigenvalue.

## 4.1. Spectrum of the Double-Layer Operator: Deflation and Iteration

The double-layer operator $\mathscr{K}$ has eigenvalues of the form[3,8]

$$\lambda = \frac{E^{(i)} - E^{(o)}}{E^{(i)} + E^{(o)}} \tag{34}$$

where $E^{(i)}$ and $E^{(o)}$ are the energy dissipation rates inside and outside the surfaces, of the velocity field produced by the eigenfunction acting as a double-layer density. The energy dissipation rates are nonnegative real numbers, and therefore the eigenvalues of $\mathscr{K}$ lie on the real line between $-1$ and 1 (inclusive), with the end points of the spectrum corresponding to a zero velocity field on one side of the particle surface. For the $N$-particle problem, the dimension of the eigenspaces for the eigenvalues at $-1$ and 1 are $6N + C$ and $N + 6C$, respectively, where $C$ is 0 or 1 depending on whether the domain is unbounded or bounded by a container wall. Thus, for the iterations to converge, these eigenvalues must be moved inward. We will devise a procedure that actually moves them to zero (a procedure known as deflation). We mention in passing that the better known electric double-layer operator, which plays an analogous role in the solution of the Laplace equation, has eigenvalues only on one side of the origin (see for example, the exercises in Chapter 7 of Friedman[13]), so the deflate-and-iterate approach given below is even easier for the Laplace equation.

We digress briefly to consider an analytical example, before proceeding with the general algorithm. For the case when $S$ is the surface of a single

isolated sphere, the spectrum of $\mathscr{K}$ has been determined analytically.[4] The explicit result for the eigenvalues are:

$$\text{Branch 1:} \quad (n \geqslant 1) \quad \lambda_n = \frac{-3}{2n+1} \tag{35}$$

$$\text{Branch 2:} \quad (n \geqslant 1) \quad \lambda_n = \frac{-3}{(2n-1)(2n+1)} \tag{36}$$

$$\text{Branch 3:} \quad (n \geqslant 0) \quad \lambda_n = \frac{3}{2n+1} \tag{37}$$

with the degeneracy of $2n+1$ at the index $n$ for each branch. After the eigenvalues at $\pm 1$ are removed by deflation, the iterations converge to three significant figures after five iterations, because the spectral radius of the deflated system is only 3/5.

Some completion procedures increase the spectral radius. We have developed[4] the completion procedure for the double layer which also simultaneously shifts all eigenvalues $\lambda = -1$ (i.e., the eigenvalues associated with the eigenspace corresponding to the null space of $1 + \mathscr{K}$) to the origin, by a procedure known as Wielandt's deflation. In general, the term deflation refers to algorithms for moving eigenvalues to the origin. Wielandt's deflation uses only the eigenvectors of the operator, and not those of the adjoint. (For our problem, at $\lambda = -1$, the eigenfunctions of $\mathscr{K}$ are known analytically, since these are the rigid-body motion null solutions, while the eigenfunctions of $\mathscr{K}^*$ are unknown.) The major disadvantage of Wielandt's deflation is that the eigenvectors of the deflated system are unknown. Consequently, Wielandt's deflation is usually a *sequential* operation, with deflation interlaced with eigenvector calculations. However, by using an orthonormal basis, the entire eigenspace can be deflated in simultaneously.[4] To execute Wielandt's deflation for an $N$-particle system in unbounded flow, we complete the double layer and obtain a unique solution by requiring

$$-\mathbf{U}^{(\alpha)} = \sum_{i=1}^{3} -U_i^{(\alpha)} \mathbf{e}_i = \sum_{i=1}^{3} \boldsymbol{\varphi}^{(i,\alpha)} \int_{S_\alpha} \boldsymbol{\varphi}^{(i,\alpha)} \cdot \boldsymbol{\varphi} \, dS \tag{38}$$

$$-\boldsymbol{\omega}^{(\alpha)} \times (\mathbf{x} - \mathbf{x}_\alpha) = \sum_{i=4}^{6} \boldsymbol{\varphi}^{(i,\alpha)} \int_{S_\alpha} \boldsymbol{\varphi}^{(i,\alpha)} \cdot \boldsymbol{\varphi} \, dS \tag{39}$$

where $\{\boldsymbol{\varphi}^{(i,\alpha)}\}$, $i = 1,..., 6$, $\alpha = 1,..., N$, form an *orthonormal* basis for the null space. On each particle surface (fix $\alpha$) the first three null functions are, except for constant scale factors, simply the unit coordinate vectors, while

the last three are rotations about the coordinate axes, again with constant scale factors (the moment of inertia per unit mass, about those axes). We substitute the expression for $\mathbf{U}^{(\alpha)}$ and $\boldsymbol{\omega}^{(\alpha)}$ into the boundary integral equations (14). In operator notation, we see that $\mathscr{K}$ is replaced by

$$\mathscr{K}' = \mathscr{K} + \sum \boldsymbol{\varphi}^{(i,\alpha)} \langle \boldsymbol{\varphi}^{(i,\alpha)}, \bullet \rangle \tag{40}$$

Each $\boldsymbol{\varphi}^{(i,\alpha)}$ is still an eigenfunction, but now its eigenvalue is 0. Generalizing this process to all particle surfaces, we shift all $6N$ eigenvalues of $\mathscr{K}$ at $-1$ to 0. This can be visualized most readily in the Jordan canonical form of the system. The following example, with matrices from Karrila *et al.*,[4] illustrates the essential ideas behind the method. The addition of the term

$$\sum_i \boldsymbol{\varphi}^{(i,\alpha)} \langle \boldsymbol{\varphi}^{(i,\alpha)}, \bullet \rangle$$

can be described pictorially as follows:

$$\begin{pmatrix} -1 & 0 & 0 & 0 & \cdots & 0 \\ 0 & -1 & -1 & 0 & \cdots & 0 \\ 0 & 0 & -1 & 0 & \cdots & 0 \\ 0 & 0 & 0 & \lambda_7 & \cdots & 0 \\ \vdots & \vdots & \vdots & \vdots & & \vdots \\ 0 & 0 & 0 & 0 & \cdots & 1 \end{pmatrix} + \sum_i \boldsymbol{\varphi}^{(i,\alpha)} \langle \boldsymbol{\varphi}^{(i,\alpha)}, \bullet \rangle$$

$$= \begin{pmatrix} 0 & x & x & X & \cdots & X \\ x & 0 & x & X & \cdots & X \\ x & x & 0 & X & \cdots & X \\ 0 & 0 & 0 & \lambda_7 & \cdots & 0 \\ \vdots & \vdots & \vdots & \vdots & & \vdots \\ 0 & 0 & 0 & 0 & \cdots & 1 \end{pmatrix} \tag{41}$$

Wielandt deflation destroys the Jordan form, but the matrix remains *block triangular.*

The 3 by 3 blocks on the upper left corner of these matrices represent schematically the $6N$ by $6N$ blocks of the actual system of equations. This entire block gets mapped to zero, i.e., the $x$'s are zero, *if and only if an orthonormal basis is used for the deflated eigenspace.* It is important to do so, since with $x$'s zero, the deflated matrix will be *triangular* as opposed to just block triangular, and the eigenvalues may be read off the diagonal. Note that the eigenvalues of a block-triangular matrix are given by those

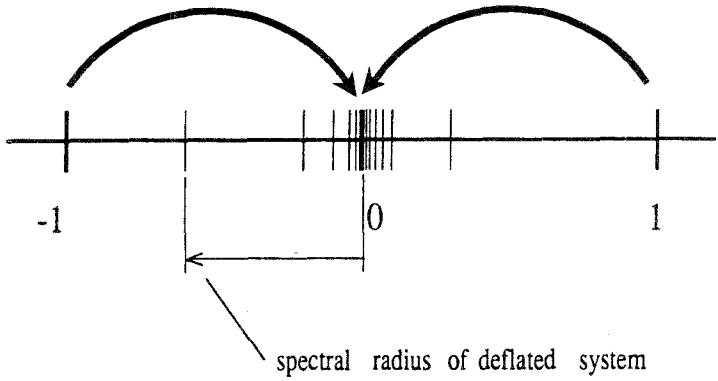


Fig. 3. The discrete spectrum of the compact operator $\mathscr{K}$. The origin is a limit point.

of the diagonal blocks and this implies that the remaining eigenvalues not at $-1$ have not been shifted. Finally, we stress that the Jordan canonical form is used only to simplify the exposition; in actual computation, we do not need to find the Jordan form. (Our illustration applies to the original system, since similarity transformations to and from the Jordan form preserve eigenvalues.)

The double-layer operator is compact[13,14] and so a central result from the spectral theory of compact operators applies: the set of eigenvalues (spectrum) of a compact operator is discrete, with at most one limit point, which, if present, can be only at the origin. A typical spectrum for the double-layer operator $\mathscr{K}$ is shown in Fig. 3. After deflation of the eigenspace at $-1$, we may use relaxation methods to solve the system, since an appropriate choice of the relaxation parameter yields a spectral radius of less than one. However, an even more efficient iterative scheme is obtained by first deflating the eigenvalues at $\lambda = 1$, as shown in Fig. 3. This is possible since the eigenfunctions of $\mathscr{K}^*$ are also known analytically at $\lambda = 1$.[4]

The explicit procedure for deflating the eigensystem at $\lambda = 1$ is as follows. Let $\tilde{\varphi}$ be an eigenvector for the eigenvalue $\lambda$ of the adjoint, denoted by $\mathscr{K}^*$. For the discretized system,

$$\mathscr{K}^*(\tilde{\varphi}) = \lambda\tilde{\varphi} \qquad \text{or} \qquad [\mathscr{K}^*]^{-1}(\tilde{\varphi}) = \lambda^{-1}\tilde{\varphi} \tag{42}$$

Then

$$(\mathscr{K} + q\tilde{\varphi}\tilde{\varphi}')\mathscr{K}^{-1} = 1 + q([\mathscr{K}^*]^{-1}\tilde{\varphi}\tilde{\varphi}')' = 1 + \frac{q}{\lambda}\tilde{\varphi}\tilde{\varphi}' \tag{43}$$

so that

$$\mathscr{K}^{-1} = (\mathscr{K} + q\tilde{\varphi}\tilde{\varphi}')^{-1}\left(1 + \frac{q}{\lambda}\tilde{\varphi}\tilde{\varphi}'\right) \tag{44}$$

where $q$ is an arbitrary parameter which we shall set presently. Therefore, the problem $\mathscr{K}(x)=b$ has the solution

$$x=(\mathscr{K}+q\tilde{\varphi}\tilde{\varphi}')^{-1}\left(1+\frac{q}{\lambda}\tilde{\varphi}\tilde{\varphi}'\right)b \tag{45}$$

so that the same solution is obtained from the system

$$\mathscr{K}(x)+q\tilde{\varphi}\langle\tilde{\varphi},x\rangle=b+\frac{q}{\lambda}\tilde{\varphi}\langle\tilde{\varphi},b\rangle \tag{46}$$

If we set $q^{-1}=-|\tilde{\varphi}|^2$, then the eigenvalue $\lambda=1$ in the original problem is now at 0 in the modified system of equations, while all other eigenvalues remain fixed.

In the Jordan canonical form, the "before" and "after" pictures of the deflation of $\lambda=1$ are as follows:

$$[\mathscr{K}]=\begin{pmatrix}0&0&0&X&\cdots&X\\0&0&0&X&\cdots&X\\0&0&0&X&\cdots&X\\0&0&0&\lambda_7&\cdots&0\\\vdots&\vdots&\vdots&\vdots&&\vdots\\0&0&0&0&\cdots&1\end{pmatrix}\rightarrow[\mathscr{K}-|\tilde{\varphi}|^{-2}\tilde{\varphi}\tilde{\varphi}']$$

$$=\begin{pmatrix}0&0&0&X&\cdots&Y\\0&0&0&X&\cdots&Y\\0&0&0&X&\cdots&Y\\0&0&0&\lambda_7&\cdots&Y\\\vdots&\vdots&\vdots&\vdots&&\vdots\\0&0&0&0&\cdots&0\end{pmatrix}$$

The placement of $Y$'s in the last column indicates that these elements are the ones that are modified. This completes the discussion on the deflation procedure for $N$ particles in unbounded flow. The theory for flow domains bounded by a container is considerably more involved and the deflation procedure is best described using projections onto the eigenspaces of $\mathscr{K}$.[5] However, the final result there is also readily implemented numerically.

The success of our iterative numerical method depends on the value taken by the spectral radius. We have observed numerically the (initially)

surprising but desirable result that the $N$-sphere system has essentially the same spectral radius as the single sphere. In other words, hydrodynamic interactions introduce only weak perturbations of the spectrum, thus opening the way for a number of tailor-made iterative algorithms. The origin of this fortuitous phenomenon is described in the next section.

## 4.2. Spectral Perturbations due to Hydrodynamic Interactions

Hydrodynamic interactions induce a split in the spectrum, analogous to the situation with energy levels in quantum mechanics. Here, however, the spectral radius undergoes only a minor perturbation, even for relatively close surfaces, because the eigenfunctions (particle double-layer densities) interact rather weakly as force-free and torque-free disturbances. For interactions between two particles of arbitrary shape separated by a distance $R$, the spectral radius is perturbed from the one-particle values by at most a term of order $R^{-3}$. The double-layer potentials in the eigenvalue problem correspond to force-free particles, so their decay persists at most by $R^{-2}$, in effect appearing as stresslet fields far away from the particle. The reflections at the other particle are also force-free, so only the gradients of the incident field are relevant, thus leading to the $O(R^{-3})$ perturbation.

The situation for sphere–sphere interactions is even more fortuitous. The five degenerate eigenvalues at $-3/5$ that determine the spectral radius of the single sphere correspond to a quadrupole field, whereas the stresslet field correspond to the unimportant eigenvalues at $-1/5$. Explicit proofs are given in Karrila *et al.*[4] The quadrupole field decays as $R^{-3}$, and upon reflection at the other particle, excite only the quadrupole moment. The Faxén law for this moment involves the second derivative of the incident field,[5] thus leading to the extremely weak $O(R^{-5})$ perturbation. This simple argument for the sphere–sphere interactions is now verified by direct calculation.

Consider two equal spheres with their centers $\mathbf{x}_1$, $\mathbf{x}_2$ separated by a distance $R = |\mathbf{x}_1 - \mathbf{x}_2|$ as before. If $R$ is very large, we may neglect interactions between the two and the eigensystem would simply be that obtained by superposition of the results for each sphere. The question is what happens as we decrease $R$.

At this point, it may be helpful to draw an analogy with a similar problem for quantum mechanics, viz., the mixing of atomic orbitals to create molecular orbitals. For example, as shown in Fig. 4, we can mix the $p_z$ orbitals of two widely-separated atoms in either a *bonding* $(\psi_1 - \psi_2)$ or *antibonding* $(\psi_1 + \psi_2)$ fashion. The former builds up electron densities in the overlap region, while the latter creates an electron-deficient region near the newly created node.

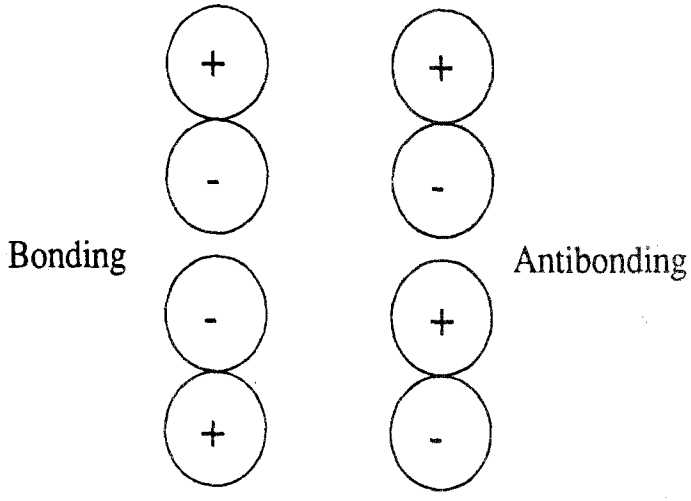


Fig. 4. Bonding and antibonding combinations of $p_z$ orbitals.

With these ideas in mind, we write the eigenfunctions for the two-sphere system as:

$$\varphi_n(1) = \varphi_n^{(0)}(1) + \sum_{j \neq n} c_{nj} \varphi_j^{(0)}(1) \qquad \text{on} \quad S_1 \tag{47}$$

$$\varphi_n(2) = \varphi_n^{(0)}(2) + \sum_{k \neq n} c_{nk} \varphi_k^{(0)}(2) \qquad \text{on} \quad S_2 \tag{48}$$

where $\varphi_n^{(0)}$ are the eigenfunctions of the single-sphere problem. The eigenfunction $\varphi_k^{(0)}(2)$ as a double-layer density generates a velocity field "$\mathbf{v}_k$" outside sphere 2. The inner product between this velocity field and the basis elements on the surface of sphere 1 is an important quantity. We introduce the notation

$$\langle \boldsymbol{\varphi}_j^{(0)}(1), \mathscr{K} \boldsymbol{\varphi}_k^{(0)}(2) \rangle_1 = \int_{S_1} \boldsymbol{\varphi}_j^{(0)}(1) \cdot \mathbf{v}_k \, dS \tag{49}$$

so that *on* $S_1$,

$$\int_{S_2} \mathbf{K}(\mathbf{x}, \xi_2) \cdot \boldsymbol{\varphi}_k^{(0)}(\xi_2) \, dS_2 = \sum_j \boldsymbol{\varphi}_j^{(0)}(1) \langle \boldsymbol{\varphi}_j^{(0)}(1), \mathscr{K} \boldsymbol{\varphi}_k^{(0)}(2) \rangle_1 \tag{50}$$

On the surface of sphere 1, the eigenvalue problem $\mathscr{K}(\boldsymbol{\varphi}_n) = \lambda_n \boldsymbol{\varphi}_n$ becomes

$$\lambda_n^{(0)} \boldsymbol{\varphi}_n^{(0)} + \sum_{j \neq n} c_{nj} \lambda_j^{(0)} \boldsymbol{\varphi}_j^{(0)}(1) \pm \sum_j \langle \boldsymbol{\varphi}_j^{(0)}(1), \mathscr{K} \boldsymbol{\varphi}_k^{(0)}(2) \rangle_1 \, \boldsymbol{\varphi}_j^{(0)}(1)$$

$$= \lambda_n \boldsymbol{\varphi}_n^{(0)} + \lambda_n \sum_{j \neq n} c_{nj} \boldsymbol{\varphi}_j^{(0)}(1) \tag{51}$$

The first and second terms on the left-hand side of this equation result from the fact that the $\varphi_j^{(0)}$ are eigenfunctions of $\mathscr{K}$ restricted to $S_1$, with eigenvalues $\lambda_j^{(0)}$. Looking at each mode, we find the following set of equations:

$$\text{For } j=n: \qquad \lambda_n = \lambda_n^{(0)} \pm \langle \varphi_j^{(0)}(1), \mathscr{K}\varphi_k^{(0)}(2)\rangle_1 \tag{52}$$

$$\text{For } j\neq n: \qquad c_j = \frac{\pm\langle \varphi_j^{(0)}(1), \mathscr{K}\varphi_k^{(0)}(2)\rangle_1}{\lambda_n^{(0)} - \lambda_j^{(0)} \pm \langle \varphi_j^{(0)}(1), \mathscr{K}\varphi_k^{(0)}(2)\rangle_1} \tag{53}$$

Here, $\pm$ denotes the sign used to construct the base solution, $\varphi_n^{(0)}(1) \pm \varphi_n^{(0)}(2)$.

We have arrived at the desired result. The eigenvalues of the two-sphere system are given by those of the single-sphere problem, plus a small perturbation proportional to the interaction factor $\langle \varphi_j^{(0)}(1), \mathscr{K}\varphi_k^{(0)}(2)\rangle_1$, which we evaluate presently with an addition theorem. But first, we may estimate the $R$ dependence of the spectral radius with this limited information. From the discussion for the single sphere, we know that the dominant eigenfunctions (the ones with eigenvalue $-3/5$) generate a Stokes quadrupole field, which decays as $|\mathbf{x}-\mathbf{x}_2|^{-3}$. The fact that $j=n$ determines the eigenvalue shift implies that we need the quadrupole moment induced on sphere 1, as claimed earlier.

We require the following addition theorem for Stokes flow[15,16]:

$$\langle \varphi_{n'm'}^{(0)}(1), \mathscr{K}\varphi_{nm}^{(0)}(2)\rangle_1 = (1+\lambda_{n'}^{(0)})(-1)^{m+n}\delta_{mm'}[n(n+1)\,n'(n'+1)]^{1/2} \times \frac{\eta_{nm}}{\eta_{n'm}}\binom{n+n'}{n+m}\frac{-R^{-(n+n'+1)}}{(n+1)(n'+1)}$$

The factor of $(1+\lambda_{n'}^{(0)})$ takes into account the jump between the surface density $\varphi(\xi_2)$ on $S_2$ and the associated velocity field emanating from sphere 2. *This factor also ensures that the eigenvalues at* $-1$ *do not get shifted,* which we know has to be the case, since the eigenvalues corresponding to the null densities are always equal to $-1$, independent of the (multiparticle) geometry.

We now apply these results with $n=2$ and the eigenvalue as $\lambda_2^{(0)} = -3/5$. The perturbation result for the two-sphere system becomes

$$\begin{aligned}\lambda_2(m) &= -\frac{3}{5} \pm \frac{2}{5}\langle \varphi_{2m}^{(3)}(1), \mathscr{K}\varphi_{2m}^{(3)}(2)\rangle \\ &= -\frac{3}{5} + (-1)^{m+1}\frac{4}{15}\binom{4}{2+m}R^{-5} \\ &= -\frac{3}{5} \pm \frac{(-1)^{m+1}\,32R^{-5}}{5(m+2)!\,(2-m)!}\end{aligned}$$

We may write these results explicitly as

$$m=0: \quad \lambda=-\frac{3}{5}\left[1\pm\frac{8}{3}R^{-5}\right]$$

$$|m|=1: \quad \lambda=-\frac{3}{5}\left[1\pm\frac{-16}{9}R^{-5}\right]$$

$$|m|=2: \quad \lambda=-\frac{3}{5}\left[1\pm\frac{4}{9}R^{-5}\right]$$

where, as before, $\pm$ indicates the sign used in the mixing of the single-sphere eigenfunctions. There are five pairs, corresponding to $m=-2$, $-1$, 0, 1, 2, but two of these pairs are degenerate because $m$ and $-m$ lead to identical perturbations of the system. The end result is that there are three distinct pairs with each pair consisting of a "bonding" and "antibonding" split, thus yielding six distinct levels. As with molecular orbitals, the value of $m$ determines whether the "+" or "−" shifts the eigenvalue downward. The mathematical analysis is reminiscent of that encountered in the mixing of two $d$-atomic orbitals.

In summary, the ten degenerate eigenvalues at $-3/5$ of the decoupled

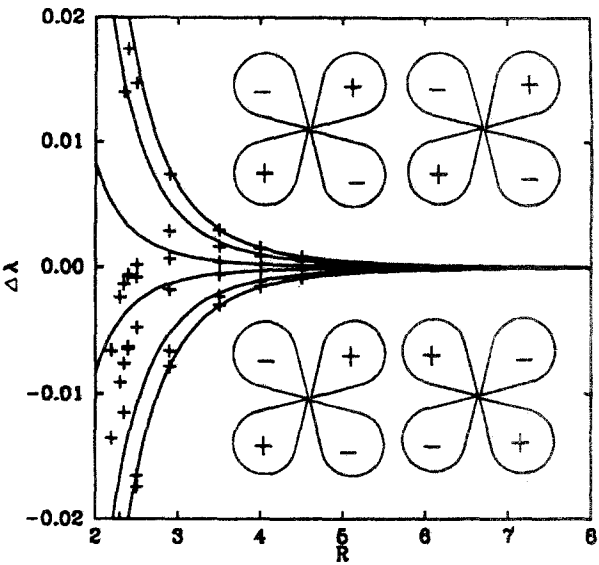


Fig. 5. Hydrodynamic interaction-induced splitting of the *outermost* eigenvalues of the two-sphere system, as a function of center–center separation $R$. Comparison of asymptotic and numerical results.

system split into a set of six distinct eigenvalues with multiplicities 1, 2, 2, 2, 2, and 1. The magnitude of the splits, as computed numerically and analytically, are in excellent agreement, as shown in Fig. 5. More importantly, in contrast with the more familiar situation in quantum mechanics, the shift in the spectrum as a result of hydrodynamic interactions is actually quite small, and thus, as stated earlier, the deflate-and-iterate scheme for multiparticle problems requires the same number of iterations as in the single-particle problem. For the sphere, according to the discussion above, the spectral radius for the two-sphere remains approximately 0.6 (the single-sphere result) at all configurations except almost touching spheres.

### 4.3. Asynchronous Iterations

The iterative solution described earlier is ideally suited for parallel machines. As shown in Fig. 6, each element of the product vector may be computed in parallel, and the algorithm can be implemented on both coarse-grained (few powerful processors linked together) and massively-parallel (many inexpensive processors linked together) designs. However, additional factors become important when we consider large (in number of unknowns) scale in the problems of actual interest. Indeed, for truly many-body interactions, the system matrix is so large that updating and

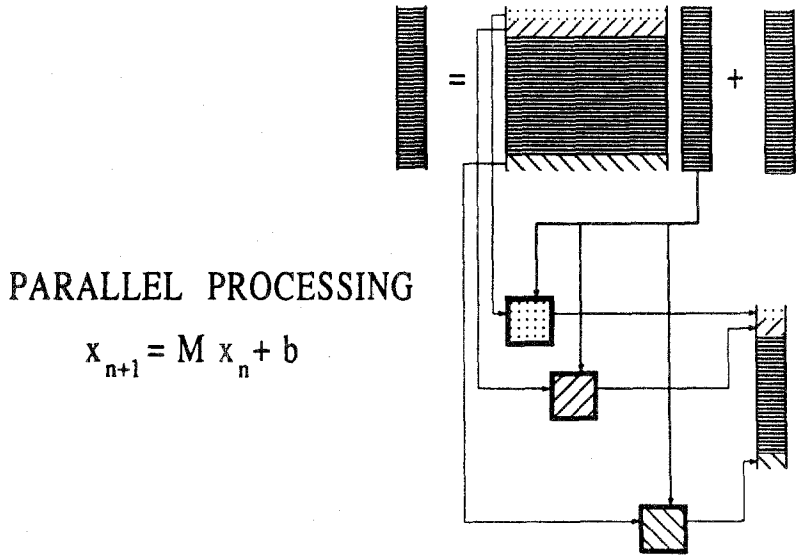


Fig. 6. Implementation of the Jacobi iteration on a parallel computer.

collation of information from the network of processors to reconstruct the unknown vector for subsequent redistribution to all becomes a nontrivial task. In other words, communication of information between processors becomes the bottleneck.

To reduce the flow of information, we replace the simple iterative scheme described above (the Jacobi iterations) with asynchronous iterations that resemble iterative schemes of the block Gauss–Seidel type. Based on physical intuition, we expect interactions between boundary elements on one particle and also those between neighboring particles to be stronger than interactions between distant particles. We perform a number of local iterations per update from a distant particle. The strategy is designed for the situation where considerable time delays can be expected for information to reach from distant regions; rather than wait and do nothing, the CDL-BIEM performs local iterations, effectively decreasing the number of *global* iterations.

Asynchronous iterations and time delays can introduce instabilities in a system that converges with Jacobi iterations. For a given matrix with spectral radius less than one, the spectral radius of a subblock may be greater than one. In this case, the local updates will diverge. In our problem, the mathematical theory comes to the rescue once again. If the matrix is divided so that all boundary elements on the same particle reside in the same block, then every submatrix formed by a subcluster of particles conforms with the CDL-BIEM spectral theory for the postdeflation many-body problem—and thus the local iterations converge.

## 5. SUMMARY AND CONCLUSIONS

We call the new method the *completed double-layer boundary integral equation method* (CDL-BIEM) because the boundary integral equation is obtained by completing a deficiency in the double-layer potential. The essence of the computational algorithm is that of an iterative solution falling in the general class of relaxation methods. The construction of the iterative scheme follows from a series of new mathematical theorems for integral representations for viscous flows.[3,4] An important feature of this method is that the system of equations remains well-conditioned with increasing size. Furthermore, on conventional, single-processor computers, computations time increases only as the square of the number of unknowns (and thus also as the square of the number of particles). An even more attractive feature is that the algorithm is parallel, so that the computation time $t$ decreases with the number of processors. To summarize these effects, even in single-particle problems, our code running on a relatively small computer such as the Micro VAX II yields accurate solutions in about the

same time as the standard boundary integral method running on a Cray. As the number of particles is increased, the new method becomes even more attractive in comparison to older methods.

CDL-BIEM is also well-suited for many-body problems. We have shown that hydrodynamic interactions induce only weak perturbations of the spectrum of the iteration operator and thus the spectral radius is essentially unchanged. This introduces great flexibility in the iterative solution of the system of equations. For truly many-body problems, we introduce processor–processor communication scheduling, or *asynchronous iterations*, to reduce the level of communication. Numerical tests of the *screening concept* from suspension and polymer theories are a natural extension. We are on the threshold of another dramatic breakthrough in computational power, perhaps rivaling that brought by the popularization of the electronic digital computer. There are design projects under way in the computer industry to produce teraflop ($10^{12}$ floating point operations per second) parallel machines. Clearly, only *parallel algorithms* will be able to take advantage of this revolution.

## ACKNOWLEDGMENTS

This work is supported by the National Science Foundation under grant CBT-8451056. Y.O.F. has also been supported by a University of Wisconsin–Madison Graduate School Fellowship.

## NOMENCLATURE

| | |
|---|---|
| $a$ | Sphere radius |
| $C$ | Container parameter |
| $E$ | Rate of energy dissipation |
| $\mathbf{E}^{\infty}$ | Ambient rate-of-strain field |
| $e$ | Unit Cartesian coordinate vector |
| $\mathbf{F}$ | Force |
| $\mathscr{G}$ | Oseen tensor (Green's dyadic for the Stokes equation) |
| $\mathscr{H}'$ | Deflated double-layer operator |
| $\mathbf{K}$ | Kernel of the double-layer operator |
| $\mathscr{K}$ | Double-layer operator |
| $M$ | Matrix |
| $N$ | Number of unknowns |
| $n$ | Number density of particles |
| $\mathbf{n}$ | Unit normal on a surface element |
| $N(\cdot)$ | Null space of an operator |
| $p$ | Pressure |
| $R$ | Separation between particle centers |
| $R(\cdot)$ | Range of an operator |
| $\mathscr{R}$ | Rotlet or point-torque |

| | |
|---|---|
| $r$ | radial spherical coordinate |
| $\mathbf{r}$ | Position vector: particle center |
| $S$ | Particle surface |
| $\mathbf{S}$ | Stresslet |
| $\mathbf{T}$ | Torque |
| $t$ | Time |
| $\mathbf{t}$ | Surface traction |
| $\mathbf{U}$ | Translational velocity |
| $\mathbf{u}$ | velocity |
| $\mathbf{v}$ | Velocity |
| $x$ | Unknown vector in linear system of equations |
| $\mathbf{x}$ | Position vector |
| $\alpha$ | Particle label |
| $\beta$ | Particle label |
| $\delta_{ij}$ | Kronecker delta |
| $\delta$ | Idemfactor |
| $\lambda$ | Eigenvalue |
| $\mu$ | Viscosity |
| $\xi$ | Position variable for surface integrals |
| $\Sigma$ | Stress field of $\mathscr{G}/8\pi\mu$ |
| $\sigma$ | Stress tensor |
| $\varphi$ | Double-layer density |
| $\Omega^\infty$ | Rotational velocity of ambient fluid |
| $\omega$ | Rotational velocity |
| $\langle \bullet, \bullet \rangle$ | Inner product (surface integral of vector dot product) |
| $\langle \bullet \rangle$ | Ensemble average |
| * | Denotes adjoint of an operator |
| † | Transpose of a matrix |
| $\perp$ | Orthogonal complement of a linear subspace |

## REFERENCES


1. J. F. Brady and G. Bossis, Stokesian dynamics, *Annu. Rev. Fluid. Mech.* **20**:111–157 (1988).
2. J. Happel and H. Brenner, *Low Reynolds Number Hydrodynamics* (Martinus Nijhoff, The Hague, 1983).
3. S. J. Karrila and S. Kim, Integral equations of the second kind for stokes flow: Direct solution for physical variables removal of inherent accuracy limitations, *Chem. Eng. Commun.* **82**:123–161 (1989).
4. S. J. Karrila, Y. O. Fuentes, and S. Kim, Parallel computational strategies for hydrodynamic interactions between rigid particles of arbitrary shape in a viscous fluid, *J. Rheol.* **33**:913–947 (1989).
5. S. Kim and S. J. Karrila, *An Introduction to Microhydrodynamics* (Butterworths, Boston, 1991).
6. H. A. Lorentz, A general theorem concerning the motion of a viscous fluid and a few consequences derived from it, *Versl. Konigl. Akad. Wetensch. Amst.* **5**:168 (1896); see also *Collected Papers* (Martinus Nijhoff, The Hague, 1937), Vol. 4, pp. 7–140.

7. G. K. Youngren and A. Acrivos, Stokes flow past a particle of arbitrary shape: A numerical method of solution, *J. Fluid Mech.* **69**:377–403 (1975).
8. F. K. G. Odqvist, Über die Randwertaufgaben der Hydrodynamik zäher Flüssigkeiten (On the boundary value problems in hydrodynamics of viscous fluids), *Math. Z.* **32**:329–375 (1930).
9. T. Tran-Cong and N. Phan-Thien, Stokes problems in multiparticle systems: A numerical method for arbitrary flows, *Phys. Fluids* **A1**:453–461 (1989).
10. H. Power and G. Miranda, Second kind integral equation formulation of Stokes' flows past a particle of arbitrary shape, *SIAM J. Appl. Math.* **47**:689–698 (1987).
11. H. Brenner, The Stokes resistance of an arbitrary particle—IV. Arbitrary fields of flow, *Chem. Eng. Sci.* **19**:703–727 (1964).
12. G. K. Batchelor, The stress system in a suspension of force-free particles, *J. Fluid Mech.* **41**:545–570 (1970).
13. A. Friedman, *Foundations of Modern Analysis* (Dover, New York, 1982).
14. D. Ramkrishna and N. R. Amundson, *Linear Operator Methods in Chemical Engineering* (Prentice-Hall, Englewood Cliffs, New Jersey, 1985).
15. D. J. Jeffrey and Y. Onishi, Calculation of the resistance and mobility functions for two unequal rigid spheres in low-Reynolds-number flow, *J. Fluid Mech.* **139**:261–290 (1984).
16. R. Schmitz and B. U. Felderhof, Friction matrix for two spherical particles with hydrodynamics interactions, *Physica* **113A**:90–102 (1982).